Control of Volatile Organic Compounds by an ac Energized Ferroelectric Pellet Reactor and a Pulsed Corona Reactor

Toshiaki Yamamoto, Kumar Ramanathan, Phil A. Lawless, David S. Ensor, J. Randall Newsome, Norman Plaks, and Geddes H. Ramsey

Abstract—**Two laboratory-scale plasma reactors (an alternating current (ac) energized ferroelectric (high-dielectric ceramic) packed bed reactor and a nanosecond pulsed corona reactor) were constructed. This study was done to develop baseline engineering data to demonstrate the feasibility of the application of plasma reactors to the destruction of various volatile organic compounds (VOC's) at ppm levels.**

Complete destruction was obtained for toluene. Conversions of methylene chloride at 95% and trichlorotrifluoroethane (known as CFC-113) at 67% were achieved for the plasma reactors used. The conversion was dependent on the mean electron energy in the reactor and was also related to how strongly halogen species were bonded with carbon.

Introduction

CONTROLLING or destroying toxic air pollutants such as volatile organic compounds (VOC's) and various chlorofluorocarbons, known collectively as CFC's, is a subject of increasing interest because of the global environmental problems of stratospheric ozone depletion and climatic changes. However, the destruction of CFC's has been regarded as difficult because of their inertness and chemical stability. Besides, the products of CFC destruction—in particular fluorine species such as HF, F_2, and chlorine compounds or any other intermediates—are difficult to treat because of their corrosiveness.

The conventional technologies for controlling VOC's and CFC's are carbon adsorption, catalytic oxidation, and thermal incineration. However, these technologies have associated problems such as cost, energy requirements, or the necessity for subsequently destroying the collected pollutant. For these reasons, a novel technology using corona-induced plasma discharge devices was investigated as an alternative technical approach to control these pollutants.

Paper IUSD 89-95, approved by the Electrostatic Processes Committee of the IEEE Industry Applications Society for presentation at the 1989 Industry Application Society Annual Meeting, San Diego, CA, October 1-5. This work was supported by the U.S. Environmental Protection Agency under Assistance Agreement EPA Cooperative Agreement CR812281. Manuscript released for publication June 18, 1991.

T. Yamamoto, P. A. Lawless, D. S. Ensor, and J. R. Newsome are with Research Triangle Institute, Center for Aerosol Technology, Research Triangle Park, NC 27709-2194.

N. Plaks and G. H. Ramsey are with the U.S. Environmental Protection Agency, Air and Energy Engineering Research Laboratory, Research Triangle Park, NC 27711.

K. Ramanathan is with Ciba-Geigy Corporation, Greensboro, NC 27419-8300.

IEEE Log Number 9106819.

Corona process applications emphasize one of two aspects of the discharge: either the ions produced or the energetic electrons producing the plasma. The ions identified depend on the polarity of the discharge and the characteristics of the gas mixture. The electron energies depend on the gas characteristics and on the method of generating the corona. In general, in an application using ions, the plasma zone will occupy a small fraction of the total process volume, whereas a process using electrons will fill most of the volume with the plasma.

Plasma chemical processes have been known to be highly effective in promoting oxidation, enhancing molecular dissociation, or producing free radicals to enhance a chemical reaction. Plasma processes have been carried out in either a high-temperature environment or at reduced pressure to provide higher electron and lower gas temperature glow discharge plasmas. A typical reactor is the silent corona reactor, which is energized by an alternating current (ac) with frequency ranging up to 40 kHz. The applications using a silent corona were for ozone production [1], enhanced combustion [2], and destroying chemical agents [3].

With the proper engineering of the corona discharge, low temperature and lower power plasma processing have been extended to atmospheric pressure applications. A narrow-gap, direct current (dc) corona discharge device with point-to-plane [4], [5] and triangle-shaped geometry [6] was developed that would decompose dimethyl methyl phosphonate (DMMP), which acted as a simulant for other gases of the same family. The power requirements for this device were considerably less than those for the silent corona device. One disadvantage of the dc corona reactors is that the electrode distance is limited to less than approximately 1.0 cm.

Streamer corona discharge energized by a fast rising time pulse voltage can produce an intensive plasma, which effectively promotes gas-phase chemical reactions. The applications were ozone generation or decomposition of nitrogen mono-oxide, sulfur dioxide, and mercury from combustion gas [7]–[9].

In this study, a laboratory-scale plasma reactor with a packed ferroelectric (high-dielectric ceramic) pellet layer (which was originally developed by Mizuno *et al.* [10]) and a nanosecond pulsed corona reactor were constructed. This study was the first attempt to develop baseline engineering data on the application of these plasma reactors to the destruction of various VOC's. Gas retention time, concentra-

0093-9994/92$03.00

tion, and corona power were varied to determine the effect on destruction efficiency using gas chromatography for each VOC.

Characteristics of Plasma Reactors and Experimental Systems

The ferroelectric packed bed reactor employed an ac power supply in conjunction with a tubular reactor packed with a ferroelectric (high-dielectric ceramic) pellet layer. The $BaTiO_3$ pellets, which are 1, 3, and 5 mm in diameter, were held within the tube arrangement by two metal mesh electrodes (2.5-cm separation) connected to a high-voltage ac power supply as shown in Fig. 1.

When external ac voltage (60 Hz) was applied across the high dielectric layer, the $BaTiO_3$ pellets (dielectric constant of 5000) were polarized, and an intense electric field was formed around each pellet contact point, resulting in partial discharge. As the applied ac voltage increased beyond the corona onset voltage, an increase of plasma activity was visible. The reactor was filled with high-energy free electrons with every half cycle. Fig. 2 shows the emission spectra of the ac packed bed reactor. The emission spectra were measured by the emission spectroscopy in the wavelength range from 200 to 800 Å. The results showed the peaks of Ti and Ba ions. These emissions may result from local heating near the contact point, where the electron and ion bombardment and electron temperature are excessively high.

Observation of the ac current waveform by an oscilloscope showed that the current was nonsinusoidal with numerous pulses with duration on the order of nanoseconds, which is equivalent to the time required for an electron to travel between the pellets (Fig. 3). These pulsing waveforms started to occur at the corona onset voltage and disappeared immediately after the ac peak voltage due to the space charge effect. A similar observation was observed by Mizuno *et al.* [11].

The pulsed corona reactor consisted of wire-cyclinder electrodes with a wire in center, where the pulsed high voltage was applied, and a grounded stainless steel tube fitted onto the glass tube, as shown in Fig. 4. The wire-to-cyclinder distance was 11.5 mm, and the effective wire length was 57 mm. A schematic diagram of the nanosecond pulse power supply is shown in Fig. 5. The pulsed reactor employed a positive dc power supply that was altered to produce a short pulse length with an extremely fast rise time, i.e., nanosecond order pulse. A capacitor C_1 was charged through resister R_1 by a high-voltage dc power supply. When the rotating spark gap reached the point of conduction, C_1 was discharged through the rotating spark gap and R_2 and R_3. This discharge current produced a voltage drop to the reactor. The rise time was determined by any inductance in the discharge path, which opposed any change in this current path, therefore increasing the rise time as inductance increased. A rotating spark gap is required for producing nanosecond pulsing because conventional thyrister control circuits are not able to produce such short pulsing.

A sharp-rise pulsed corona produces streamer corona, which has the advantage of generating free electrons while producing a limited number of ions. Electrons can be intensely accelerated to high energy levels (temperature) without raising the ion and gas temperature in such a short pulse field. The electric field can be raised to an extremely high level without causing sparking. The streamer coronas are further intensified by the fast rise time of the applied pulse voltage because of the very small space-charge suppression.

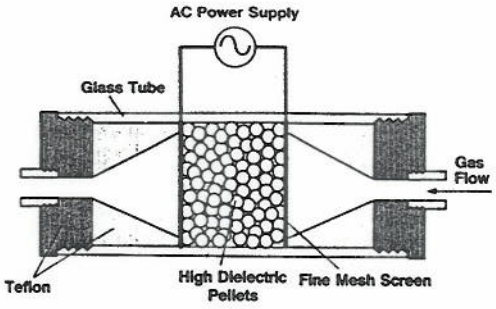

Fig. 1. Schematic of ac packed bed plasma reactor.

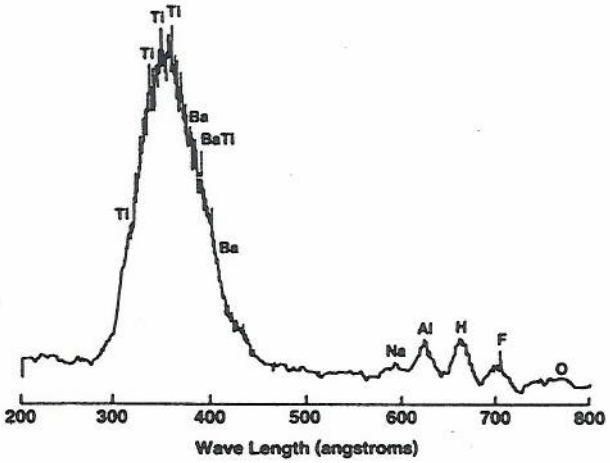

Fig. 2. Emission spectra of ac energized ferroelectric packed bed plasma reactor.

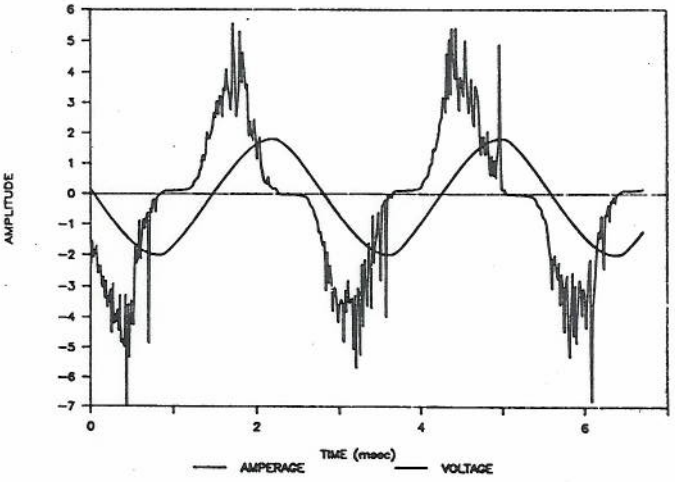

Fig. 3. Voltage-current waveforms for ac energized ferroelectric packed bed plasma reactor.

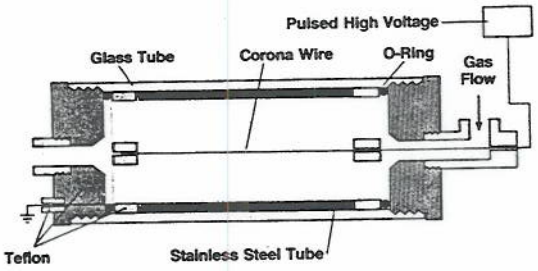

Fig. 4. Schematic of pulsed corona plasma reactor.

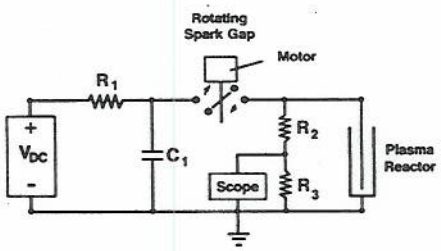

Fig. 5. Schematic of nansecond pulse power supply.

The dissociation/destruction efficiency of toluene ($C_6H_5CH_3$), methylene chloride (CH_2C1_2), and trichlorotrifluoroethane ($C_2C1_3F_3$) (CFC-113) at 50–1000 ppm in dry air were evaluated by using a packed bed plasma reactor and a nanosecond pulsed corona reactor. Gas flow rate, concentration, and reactor operating conditions (voltage, pulse repetition rate) were varied to obtain the reactor characteristics. Gas chromatography was used for evaluation of destruction efficiencies and analysis of reactant conversion for each VOC. The concentrations of CO and CO_2 were measured by a Byron Model 401 Analyzer, and the concentration of ozone was measured by Dasibi Ozone Analyzer (Model 1003AH).

Results and Discussion

ac Energized Ferroelectric Pellet Reactor

To clarify the destruction processes, relatively simple and reactive hydrocarbons, such as toluene—which was the major emission source among VOC's—were used. Fig. 6 shows the voltage-dependent destruction efficiency for toluene when the flow rate was high (800 cc/min). The effects of pellet size and toluene concentration were plotted.

It appears that the corona onset voltage decreases as the pellet diameter increases. Correspondingly, the sparking voltage increases with decreasing pellet diameter. The destruction starts to take place above the corona onset voltage, and conversion efficiency increases with increasing effective ac voltage. Destruction of 100% was obtained with the smallest pellet diameter when the applied ac voltage was 14 kV. Note that the voltage reading here was rms values. With the use of the smallest pellet size (1 mm in diameter), a much higher voltage (18 kV) and lower current were obtained, resulting in much higher destruction efficiency. This may be attributed to more uniform corona-induced plasma activities throughout the reactor volume, which was confirmed with a high-sensitivity camera connected to a videotape. In addition,

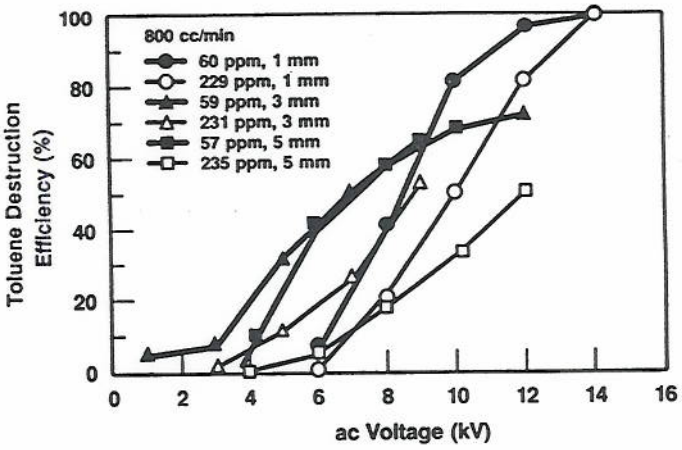

Fig. 6. Toluene destruction efficiency for ac packed bed reactor when flow rate is 800 cc/min.

higher efficiencies were obtained at the lower concentration (57–60 ppm) than at the higher concentration (229–235 ppm) for all pellet sizes tested.

The destruction efficiency for toluene when the flow rate was low (200 cc/min) is shown in Fig. 7. Almost complete destruction was attained with smaller pellet size and lower operating voltages. The trends showed that the pellet size is smaller and the concentration is lower, the destruction efficiency will be higher. It is clear from Figs. 6 and 7 that flow rate has a significant effect on the destruction efficiency.

Toluene mostly decomposed into CO_2, H_2O, and CO. However, the production of CO_2 was almost zero at lower voltages, and a small fraction of CO_2 was formed only near the sparking potential. The CO production was plotted against applied ac voltage as a function of pellet size (see Fig. 8) when the flow rate was low (200 cc/min) and the toluene concentration was high (229–235 ppm). The CO concentration reached 700 ppm for all pellet sizes. In addition, the CO concentration was proportionally lower for lowertoluene concentrations. When the flow rate was high (800 cc/min) and the toluene concentration was high, the CO concentration became pellet-size dependent—higher CO concentration resulted from smaller pellet sizes.

Fig. 9 shows the destruction efficiency for an ac-energized ferroelectric packed bed reactor with a pellet size of 3 mm. The destruction efficiency was plotted as a function of flow rate (100, 200, and 500 cm^3/min) when the concentration was maintained at 500 ppm. When the flow rate was set at 200 cm^3/min, the effect of concentration was investigated. Maximum destruction attained was 61%, and the conversion decreased with increased flow rate (decreasing residence time) and higher concentration. A higher desruction was obtained when the smaller pellet size (1 mm) was used.

The ozone concentrations in air with increasing and decreasing voltages are presented in Fig. 10. Note that the ozone concentration reached peak value at voltages of 8 to 10 kV and then decreased with increasing voltage. In the presence of methylene chloride (CH_2C1_2), the ozone concentration peak was shifted to a lower voltage, and the ozone concentration was significantly reduced at the same

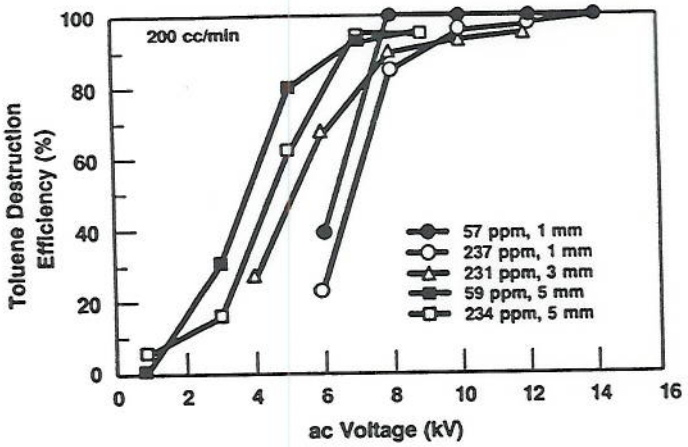

Fig. 7. Toluene destruction efficiency for ac packed bed reactor with a flow rate of 200 cc/min.

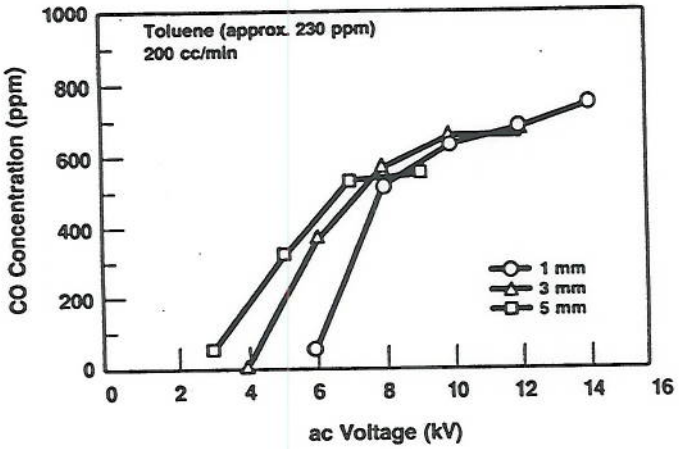

Fig. 8. CO production for ac packed bed reactor.

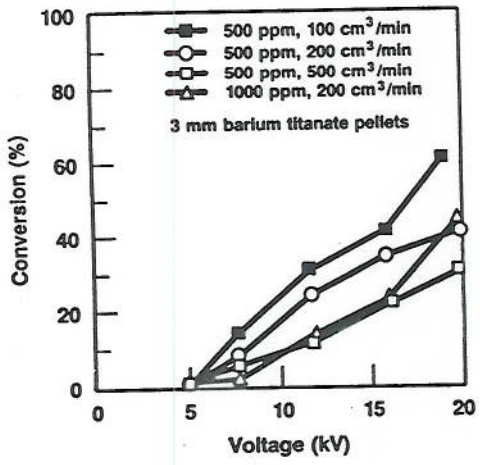

Fig. 9. Methlene chloride destruction efficiency for ac energized ferroelectric packed bed plasma reactor.

time. When the flow rate was further reduced, the peak value of ozone concentration shifted further to the right.

$BaTiO_3$ pellets with smaller size (1.5 mm in diameter) but higher porosity were used as a packed bed material.

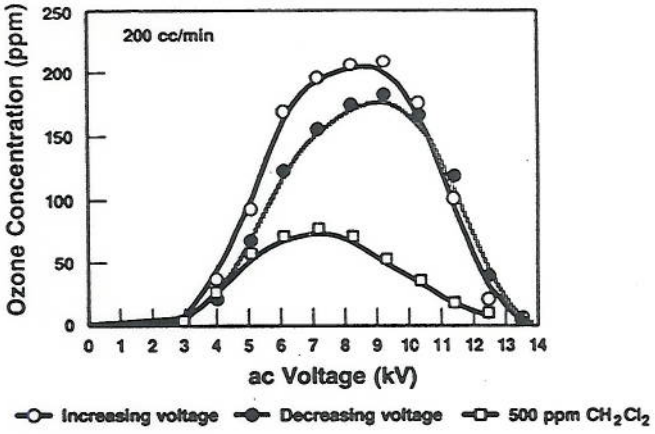

Fig. 10. Ozone concentration in air for ac packed bed reactor.

Although higher voltage and lower current were obtained, the plasma became unstable with time, resulting in lower destruction efficiency. When the pellets were replaced with 3-mm-diameter glass spheres (dielectric constant of 4), nanosecond pulsed waveforms were no longer observed, resulting in no destruction of hydrocarbons. This implies that the molecular decomposition is strongly associated with electron activity.

Nansecond Pulsed Corona Reactor

Fig. 11 is a plot of the destruction efficiency of toluene (50 ppm) against pulse repetition rate in pulses per second (pps) when the residence time was 1.5 s. When the applied voltage was the maximum (22.0 kV), which was limited by the power supply, 100% conversion was obtained with 110 pps or more. The efficiency sharply dropped as pps and voltage were further decreased. Voltages below 18.0 kV caused no sparking at the rotating spark-gap distance used. Ozone concentrations were also measured with 50 ppm of toluene and were as high as 220 ppm. In general, ozone concentration increased with applied voltage and pulse repetition rate.

Fig. 12 shows the effect of the residence time on the conversion efficiency for toluene as a function of pulse energy. Above 2.5 s residence time, complete conversion was achieved regardless of pps and pulse voltage. Pulse repetition rate and pulse voltage (or pulse input energy) became crucial factors when the residence time was shorter than approximately 2.5 s.

The destruction efficiency for methylene chloride (CH_2Cl_2) is plotted against pps in Fig. 13 for two voltage and concentration levels when the residence time was 7.9 s. Because the chlorine in methylene chloride is strongly bonded with carbon, it is much more stable chemically than toluene, and it is expected that higher electron energies are necessary to decompose methylene chloride. As expected from the bonding energies argument, only 95% conversion was achieved with higher pps and pulsed voltage. The effect of concentration was not significant for the higher operating voltages (22.0 kV), but much higher conversion was obtained at the lower concentration for the lower operating voltage

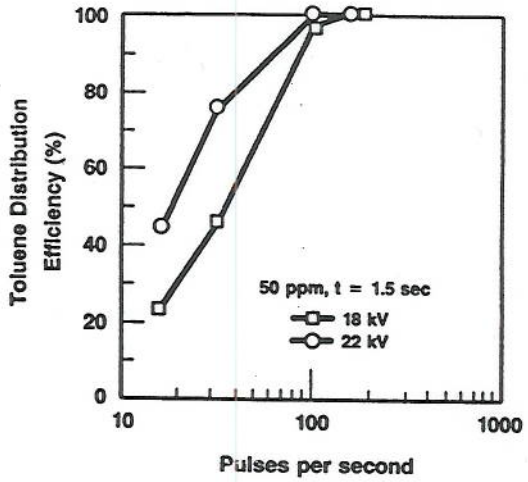

Fig. 11. Toluene destruction efficiency for pulsed corona reactor.

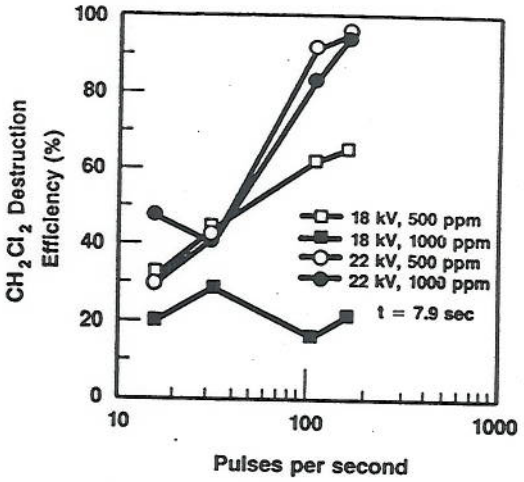

Fig. 13. CH_2Cl_2 destruction efficiency for pulsed corona reactor.

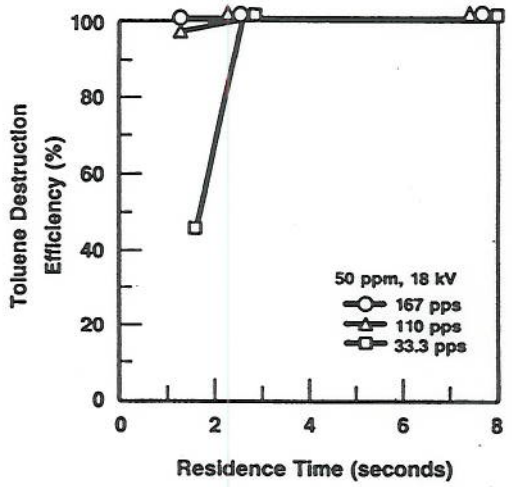

Fig. 12. Effect of residence time on toluene destruction as a function of pulse energy.

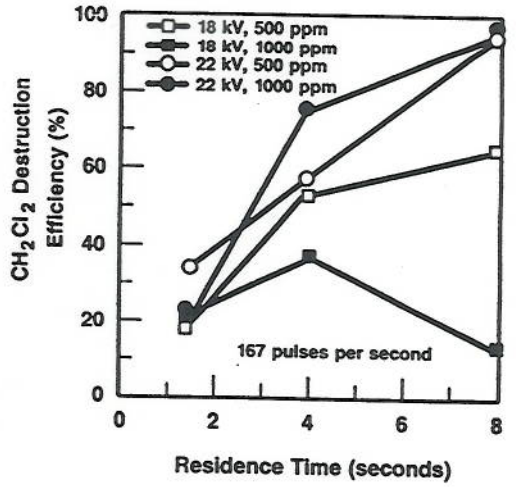

Fig. 14. Effect of residence time on CH_2Cl_2 destruction as a function of pulse energy.

(18 kV). The electron energies were not sufficiently high to yield significant conversion when operating with lower pulsed voltages and pulse repetition rates.

Fig. 14 presents the effect of the residence time on the conversion of methylene chloride. As the residence time and pulse voltage increased, the methylene chloride conversion increased. Approximately 95% conversion was obtained with 7.9 s retention time for both high and low concentrations.

Fig. 15 depicts the destruction efficiencies for two different concentration levels (500 and 1000 ppm) of CFC 113 when the retention time was 7.9 s. The destruction efficiency increased with increased pulse repetition rate for all operating cases. Higher conversion was achieved with higher pulse voltage. The maximum efficiency obtained was 67% with 500 ppm and 7.9 s residence time. This was predictable because chlorine and fluorine in CFC-113 are more strongly bonded and stable than in methylene chloride. The concentration dependence of conversion was also shown. As seen with other VOC's, higher destruction was obtained with lower concentration.

The effect of the residence time on CFC-113 conversion is shown in Fig. 16. Although a maximum efficiency of only

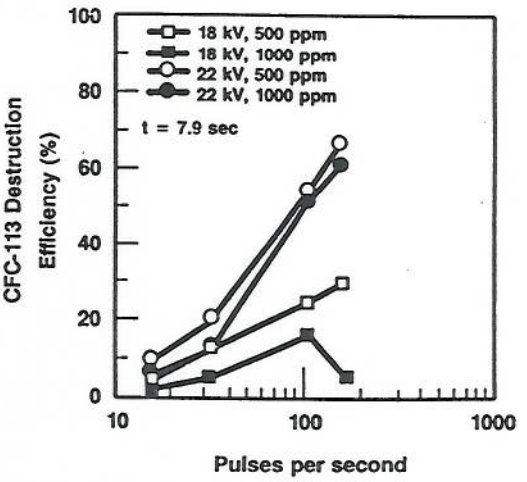

Fig. 15. CFC-113 destruction efficiency for pulsed corona reactor.

65% was achieved, it is believed that much higher efficiencies could be attained by optimizing the power supply with higher voltage and pulse rate. The present pulser is limited by pulse repetition rate and power supply voltage. Appar-

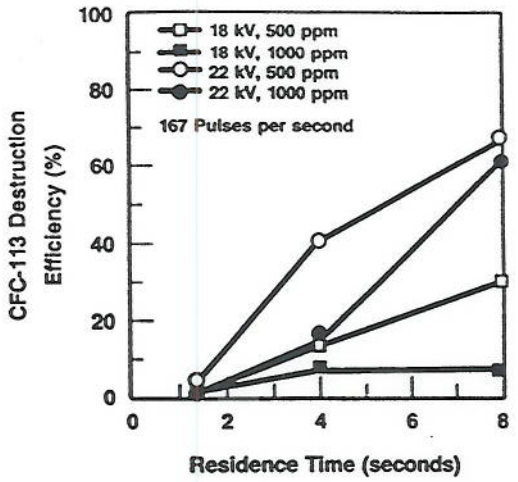

Fig. 16. Effect of residence time on CFC-113 destruction as a function of pulse energy.

ently, much higher electron energies are required to achieve improved conversion. A dark brown powder-like deposit and high-molecular-weight compound like tar was deposited on the reactor electrode and surface. However, the reaction products have not yet been identified.

Conclusions

Laboratory-scale plasma reactors such as the ac energized ferroelectric packed bed reactor and the nanosecond pulsed corona reactor were developed to evaluate the destruction efficiency of various VOC's at ppm concentrations. A 100% destruction rate was obtained for toluene. A conversion rate of 95% for methylene chloride and 67% for CFC-113 were achieved for the present design of plasma reactors. The conversion rate may be dependent on the electron energies in the reactor and may also be related to how strongly halogen species were bonded with carbon.

Acknowledgment

The work described in this paper has not been subjected to the Environmental Protection Agency's required peer and administrative review and, therefore, does not necessarily reflect the reviews of the Agency. No official endorsement should be inferred.

References

[1] S. Masuda, K. Akutsu, M. Kuroda, Y. Awatsu, and Y. Shibuya, "A ceramic-based ozonizer using high frequency discharge," in *Proc. IEEE/IES 1985 Ann. Conf.* (Toronto, Canada), Oct. 1985, pp. 1351–1358.

[2] T. Inomata, S. Okazaki, T. Moriwaki, and M. Suzuki, "Brief communication: The application of silent electric discharges to propagating flames," *Combustion Flame*, vol. 50, pp. 361–363, 1983.

[3] J. P. Gilman, J. G. Birmingham, and R. R. Moore, "Acetonitrile as a simulant for cyanide compounds for plasma testing," in *Proc. 1985 Sci. Conf. Chemical Defense Res.*, 1986, p. 435.

[4] P. M. Castle, I. E. Kanter, P. K. Lee, and L. E. Kline, "Corona glow detoxification study," Westinghouse Corp. Final Rep., Contract DAAA 09-82-C-5396, 1984.

[5] T. Yamamoto, P. A. Lawless, and L. E. Sparks, "Narrow-gap point-to-plane corona with high velocity flows," *IEEE Trans. Industry Applications*, vol. 24, no. 5, pp. 934–939, Sept./Oct. 1988.

[6] ——, "Triangle-shaped dc corona discharge device for molecular decomposition," *IEEE Trans. Industry Applications*, vol. 25, no. 4, pp. 743–749, July/Aug. 1989.

[7] A. Mizuno, J. S. Clements, and R. H. Davis, "A method for the removal of sulfur dioxide from exhaust gas utilizing pulsed streamer corona for electron energization," *IEEE Trans. Industry Applications*, vol. IA-22, no. 3, pp. 516–522, May/June 1986.

[8] S. Masuda, M. Sato, and T. Seki, "High efficiency ozonizer using traveling wave pulse voltage," *IEEE Trans. Industry Applications*, vol. IA-22, no. 5, pp. 886–891, Sept./Oct. 1986.

[9] S. Masuda, Y. Wu, T. Urabe, and Y. Ono, "Pulse corona induced plasma chemical process for DeNOx, DeSOx, and mercury vapor control of combustion gas," in *Proc. Third Int. Conf. Electrostat Precipitation* (Abano, Italy), Oct. 1987.

[10] A. Mizuno, A. and H. Ito, "An electrostatic precipator using a ferroelectric pellet layer for particle collection," in *Proc. IEEE/IES 1986 Ann. Conf.* (Denver, Co.), Oct. 1986, pp. 1106–1112.

[11] A. Mizuno, H. Ito, and H. Yoshida, "AC particle discharge characteristics of the electrostatic precipitator using a packed ferroelectric pellet layer," in *Proc. 1988 Inst. Electrostatics Japan*, Oct. 1988, pp. 337–340.